Energy & Environmental Science

Modulating Multi-Hole Reaction Pathways for Photoelectrochemical Water Oxidation on Gold Nanocatalysts

Journal:	*Energy & Environmental Science*
Manuscript ID	EE-ART-12-2019-004192.R1
Article Type:	Paper
Date Submitted by the Author:	21-Mar-2020
Complete List of Authors:	Zhang, Yuchao; Institute of Chemistry Chinese Academy of Sciences, Zhang, Yunlu; University of Florida, Department of Chemistry and Center for Nanostructured Electronic Materials Guo, Wenxiao; University of Florida, Department of Chemistry and Center for Catalysis Johnston-Peck, Aaron; National Institute of Standards and Technology, Hu, Yue; University of Florida, Department of Chemistry and Center for Catalysis Song, Xuening; University of Florida, Department of Chemistry and Center for Catalysis Wei, David; University of Florida, Department of Chemistry and Center for Nanostructured Electronic Materials

SCHOLARONE™
Manuscripts

Using visible sun light to promote chemical reactions (e.g., water oxidation, CO_2 reduction, and N_2 reduction) represents a unique approach for addressing the global energy crisis. However, those photochemical processes always involve multiple holes/electrons transfer and accumulation to ultimately generate stable products, which commonly exhibit slow kinetics in timescales from ~ ms to s. Therefore, elongating lifetimes of photo-excited hot carriers and revealing multi-carrier reaction pathways are essential in visible-light-driven photochemistry. In this work, we successfully demonstrated that catechol molecules adsorbed on Au/TiO2 heterostructures can trap and stabilize photo-generated hot holes on Au and further introduce a new multi-hole reaction pathway in which those long-lived catechol-trapped holes cooperate with newly generated holes on Au. The new reaction pathway enabled to boost the photoelectrochemical water oxidation on Au by one order of magnitude. Our study provided a molecular level understanding of the role of photo-generated hot holes in facilitating water oxidation, illustrating a strategy to assemble metal nanoparticles, semiconductors, and molecules to effectively separate charge carriers and harvest hot holes for driving photochemical reactions. We expected that this multi-hole cooperation pathway would be extendable to various multi-hole (or -electron) photochemical reactions at metal/semiconductor or metal/molecule interfaces.

Modulating Multi-Hole Reaction Pathways for Photoelectrochemical Water Oxidation on Gold Nanocatalysts

Yuchao Zhang,[1§] Yunlu Zhang,[1] Wenxiao Guo,[1] Aaron C. Johnston-Peck,[2] Yue Hu,[1] Xuening Song,[1] and Wei David Wei*[1]

[1] Department of Chemistry and Center for Catalysis, University of Florida, Gainesville, FL 32611, United States

[2] Center for Functional Nanomaterials, Brookhaven National Laboratory, Upton, NY 11973, United States

Abstract

Natural photosynthesis utilizes redox cascade consisting of enzymes and molecular mediators that trap and stabilize hot carriers to achieve efficient multiple charge transfer. In this aspect, great challenges are facing artificial photochemistry regarding extremely short lifetimes of photo-generated hot carriers. Herein, using Au nanoparticle photocatalysts as a model, we report that photoelectrodeposited catechol molecules on Au/TiO_2 heterostructures trap and stabilize photo-generated hot holes on Au and further introduce a new multi-hole reaction pathway in which those long-lived catechol-trapped holes cooperate with newly generated holes on Au. The new mechanism boosts photoelectrochemical water oxidation on Au by one order of magnitude. Our study illustrates a strategy to integrate metal nanoparticles, semiconductors, and molecular redox mediators to effectively separate charge carriers and harvest hot holes for driving photochemical reactions.

Main text

Numerous widely-tracked photochemical reactions, such as water oxidation and CO_2 reduction, involve multiple hole/electron transfer to ultimately generate stable products.[1-6] Multi-carrier reactions are based on long-lived hot carriers and multiple oxidations/reductions of active sites.[3-4, 6] Natural photosynthesis utilizes sophisticated redox cascade consisting of enzymes and molecular mediators (e.g., quinone)[7] to trap and transport hot carriers for achieving efficient multiple charge transfer. However, design principles for modulating multiple charge transfer in artificial hot-carrier photochemistry remain undeveloped.

Metal nanoparticle photocatalysts (MNPs, e.g., Au and Ag) boast broadly tunable optical properties coupled with catalytically active sites that offer unique opportunities for visible-light photocatalysis.[8-20] The direct interband transition and nonradiative decay of surface plasmon resonance on MNPs generate hot electron-hole pairs that are promising for trigging photochemical reactions.[8-26] However, lifetimes of those hot carriers are extremely short (~ fs to ns)[8, 10-11] when compared to the slow kinetics of multi-carrier reactions (~ ms to s).[3, 6, 9, 12, 24, 27-31] Numerous studies have used metal/semiconductor heterostructures to prolong lifetimes of hot electrons, thus improving low photocatalytic activities of reduction reactions.[32-34] Nonetheless, to date, very few works have been reported to manipulate photo-generated hot holes for extending their lifetimes to coincide with kinetically sluggish oxidation reactions.[35] It is noteworthy that photo-generated holes possess faster relaxation dynamics and lower mobility than electrons,[36-37] making it more difficult to trap and utilize them to promote the overall photochemical reaction efficiency.

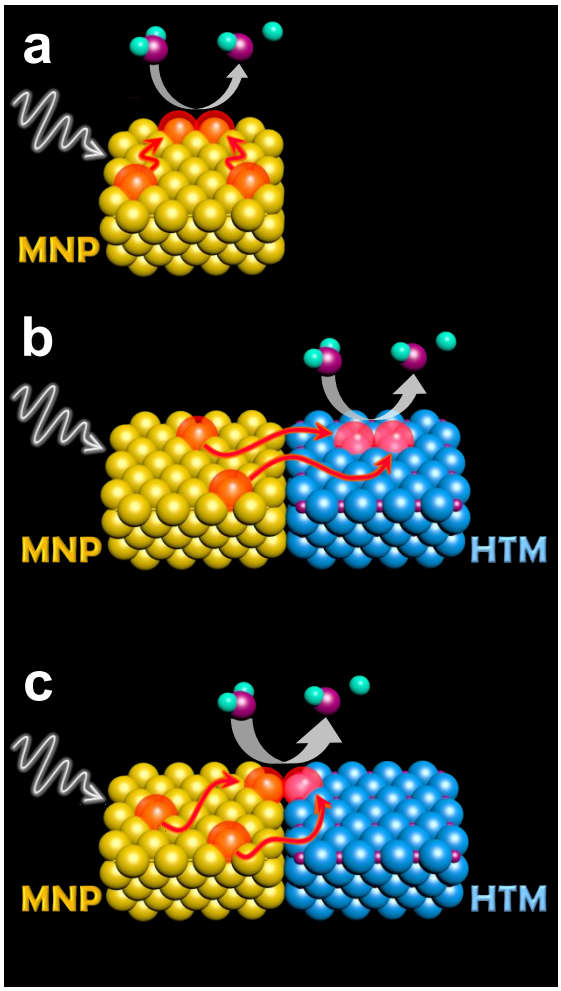

Scheme 1. Photo-induced multi-hole reaction pathways on MNPs. (**a**) Multi-hole accumulation on MNP. (**b**) Sequential oxidation pathway. Multi-hole accumulation on the hole-trapping mediator (HTM), which provides active sites for reactions. (**c**) Multi-hole cooperation pathway. The hole trapped on HTM cooperates with the subsequently generated hole on MNP to drive reactions at MNP/HTM interfaces, which circumvents the sluggish multi-hole accumulation on a single component. Red bubbles represent hot holes. The incident visible light only excites MNP but not HTM.

Long-lived hot holes lay the foundation for triggering multi-hole reactions. Directly trapping and stabilizing multiple hot holes on MNP for driving reactions (Scheme 1a) is difficult

due to extremely short lifetimes of hot holes[9, 11-12] and the high energy barrier of multi-hole accumulation.[12, 30-31] A hole-trapping mediator (HTM) then is necessary for extending lifetimes of hot holes and initiating multi-hole reactions. For instance, sequential oxidations of HTM have been reported in dye-sensitized photoelectrochemical cells.[3] Similar multi-hole reaction pathway could also exist on MNP, in which the first trapped hole encounters the second trapped hole to enable a two-hole rate-determining step (RDS) solely taking place on HTM (Sequential oxidation pathway, Scheme 1b). Alternatively, HTM-stored hot holes would cooperate with newly-generated hot holes on MNP to drive the two-hole RDS at MNP/HTM interfaces (Multi-hole cooperation pathway, Scheme 1c).

In this work, we reported that photoelectrodeposited catechol on Au/TiO_2 heterostructures stabilized photo-generated hot holes on Au under visible-light illumination and triggered a multi-hole cooperation pathway for prompting water oxidation, a typical sluggish proton-coupled four-hole reaction. Our results showed that on pristine Au/TiO_2 heterostructures, photo-generated hot holes were transferred from Au to TiO_2 for driving multi-hole reactions via the sequential pathway, but the recombination of those hot holes with hot electrons also transferred to TiO_2 severely limited the photoactivity. However, catechol molecules adsorbed on Au/TiO_2 heterostructures trapped and stabilized hot holes directly on Au and physically separated them from transferred hot electrons on TiO_2. It was further demonstrated that catechol-trapped holes coupled with those newly generated holes on Au to trigger a cooperation pathway for driving water oxidation at Au/catechol interfaces. The new mechanism was found to boost photoelectrochemical water oxidation on Au by one order of magnitude.

Results and discussion

Au/TiO_2 heterostructures were constructed by photodepositing Au nanoparticles (NPs) on TiO_2 electrodes (see the experimental section in supplementary information and Figure S1 to S4). Measuring open-circuit potentials (OCPs) in a photoelectrochemical (PEC) water-oxidation cell would identify long-lived hot holes on Au/TiO_2 heterostructures as the generation of open-circuit photovoltage ($V_{ph} = V_{light} - V_{dark}$) is known to arise from the accumulation of surface holes when electrodes consist of n-type semiconductors.[38] Indeed, Au/TiO_2 heterostructures exhibited V_{ph} of 0.2 – 0.4 V under visible-light excitation (Supplementary Note 1, Table S1, Figure S3 and S5), indicating that hot holes were accumulated on Au/TiO_2 heterostructure surfaces with extended lifetimes. To further pinpoint the exact physical location of trapped hot holes on Au/TiO_2 heterostructures, dual-working electrodes were used to measure the separated V_{ph} on Au and TiO_2 (Supplementary note 2 and Figure S6 to S9). It was found that TiO_2 exhibited a twice larger V_{ph} (~ 0.4 V) than that on Au (~ 0.2 V) (Figure 1a and Figure S8), strongly suggesting that transferred hot holes were accumulated on TiO_2. Further isotope effect on V_{ph} demonstrated that photo-generated hot holes were transferred from Au to TiO_2 via a proton-coupled process (Figure S10), which is known to have slow dynamics.[39-40] TiO_2-trapped holes were found to be released in the timescale of second (0.2 – 1.8 s, Figure 1b, Supplementary Note 3, Figure S11 to S13, and Table S2 and S3), showing that lifetimes of hot holes were extended via being trapped on TiO_2. In the unbuffered solution with pH 7.0, time constants remained unchanged with increasing potentials; while for pH 13.6, under the potential above 0.7 V_{RHE} time constants were found to increase as a function of the applied potential, implying that lifetimes of surface-trapped holes were further extended under alkaline conditions owing to circumventing the kinetically sluggish proton-coupled process.[41]

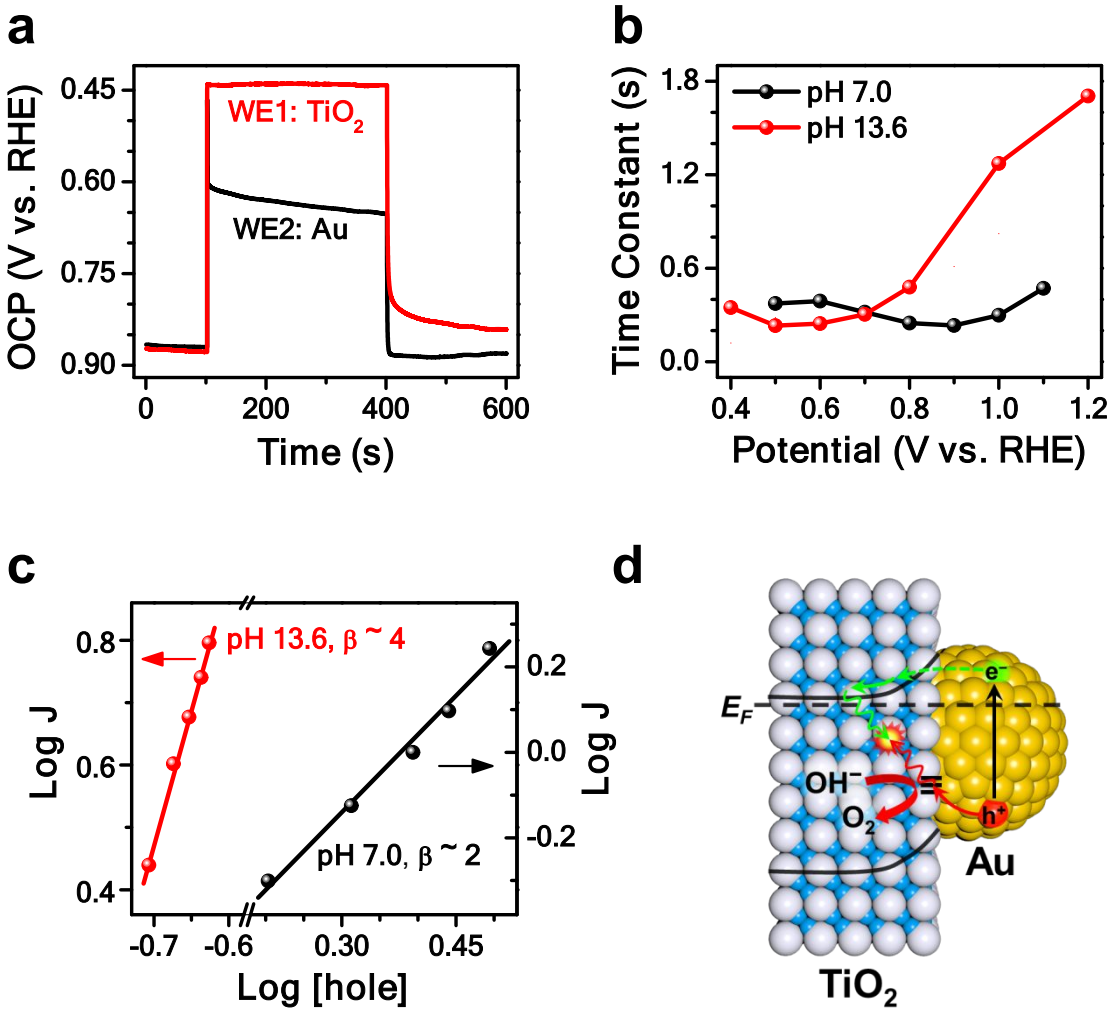

Figure 1. Visible-light-mediated hot-hole transfer on pristine Au/TiO_2 heterostructures. (**a**) V_{ph} obtained from TiO_2 (red) and Au (black) on a dual-working Au/TiO_2 electrode in the solution with pH 13.6. The light was turned on at 100 s and off at 400 s. (**b**) Trapping and releasing time constants of hot holes on TiO_2 in the unbuffered solution with pH 7.0 (black) and pH 13.6 (red). Data were calculated from electrochemical impedance spectroscopy (EIS) results measured on Au/TiO_2 heterostructures using the electric model (Figure S11). (**c**) Photocurrent densities (J in $\mu A/cm^2$) over surface-hole densities ([hole] in number of hole/nm^2) on Au/TiO_2 heterostructures in the unbuffered solution with pH 7.0 (black) and pH 13.6 (red) at 0.5 V_{RHE}. The estimation of

[hole] was shown in Supplementary note 4. (**d**) Scheme of transfer and recombination of hot carriers on Au/TiO_2 heterostructures.

Long-lived holes provide opportunities to enable multi-hole reactions such as water oxidation.[2] The reaction order for TiO_2-trapped holes in PEC water oxidation was measured to identify multi-hole reaction pathways (Supplementary Note 4, Figure S14 to S17 and Table S4). Figure 1c showed a reaction order of ~ 2 under the neutral condition (pH 7.0, black) and a reaction order of ~ 4 under the alkaline condition (pH 13.6, red), suggesting that two holes were involved in RDS of PEC water oxidation under pH 7.0 while four holes were involved under pH 13.6. This pH dependence is a typical characteristic of proton-coupled hole transfer in multi-hole reactions.[39] Under neutral conditions, TiO_2 surfaces were protonated and the slow dynamics of proton-coupled hole transfer only led to isolated surface-trapped holes (not adjacent trapped holes, Figure S17a) that underwent multiple sequential oxidations.[2] However, under alkaline conditions, the deprotonation of TiO_2 surfaces facilitated the transfer of hot holes and further-extended lifetimes of hot holes (Figure 1b) made it possible to generate two adjacent surface-trapped holes. In this scenario, those two trapped holes coupled with each other to create an alternative pathway with high efficiency for forming the rate-limiting O–O bond in water oxidation (Figure S17b).[2] For water oxidation, from the point of thermodynamics, the oxidation of OH^- ions is much easier than the oxidation of H_2O molecules.[42] Herein, the oxidation of OH^- was considered as the major contribution to the observed PEC activities (Figure S18).

Both aforementioned two-hole and four-hole reaction kinetics implied that TiO_2 alone provided active sites for water oxidation, which should follow the sequential pathway as shown in Scheme 1b. The sequential pathway required more than one hole to be trapped at HTM, but the sluggish proton-coupled hole transfer greatly hindered this process. On the other hand, it is noted

that photo-generated hot holes and electrons on Au were both transferred and trapped on TiO_2.[14, 32] Thus, it is inevitable that TiO_2 would function as an electron-hole recombination center (Figure 1d). Indeed, simultaneous photocurrent measurements on Au and TiO_2 confirmed that less than 10% of hot carriers survived from the electron-hole recombination at Au/TiO_2 interfaces under open-circuit conditions (Supplementary Note 5 and Figure S19 to S22), which severely hindered photocatalytic activities. Hence, it is necessary to develop strategies to efficiently improve physical separation of photo-generated hot electrons and holes in Au/TiO_2 heterostructures. Considering the slower mobility of holes than electrons,[36-37] it would be ideal to retain hot holes on Au while transfer hot electrons to TiO_2.

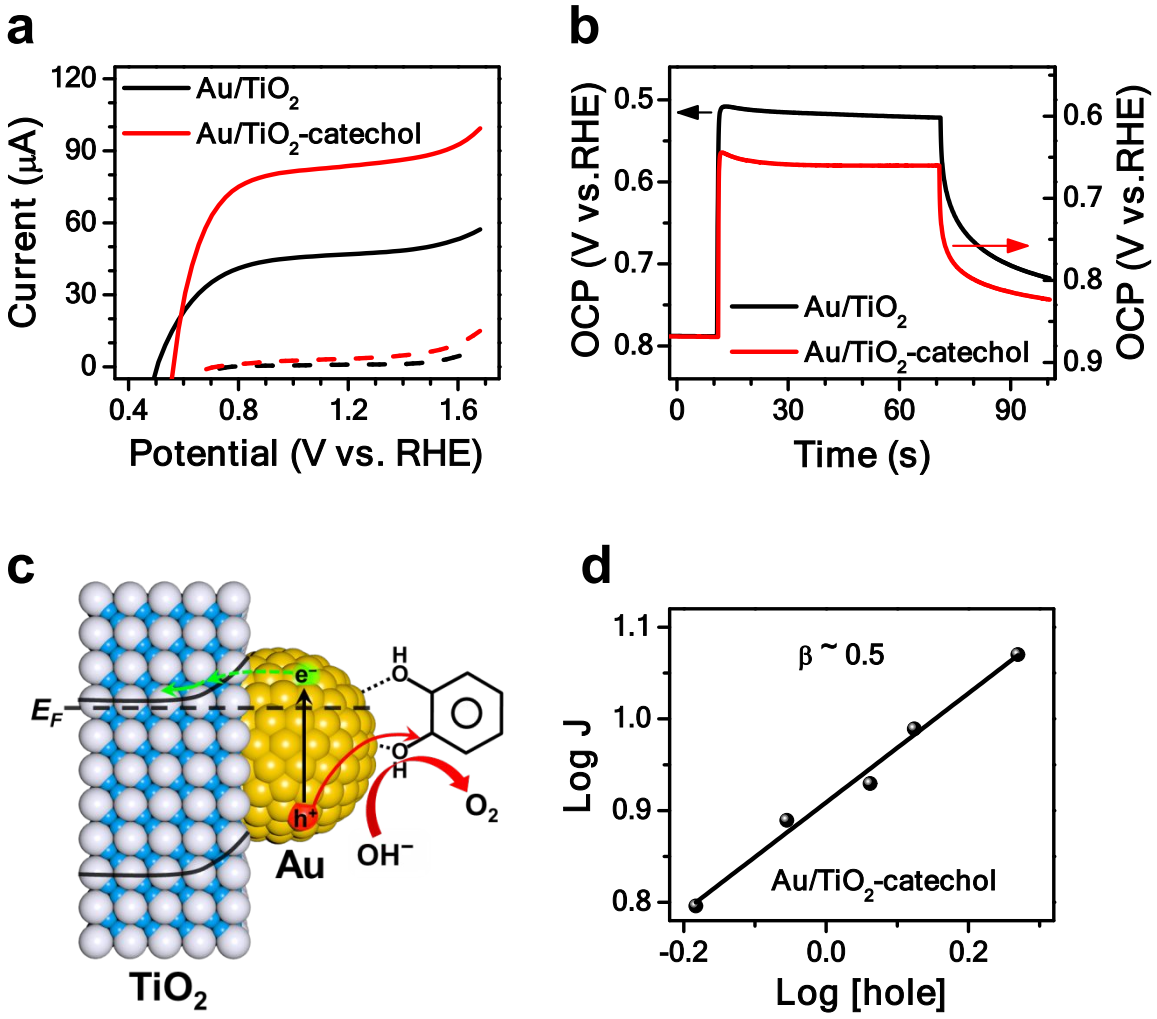

Figure 2. Catechol-mediated hot-hole trapping on Au/TiO_2 heterostructures. (**a**) LSV curves measured from pristine Au/TiO_2 heterostructures (black curves) and catechol-modified Au/TiO_2 heterostructures (red curves) under visible-light illumination (470 nm LED, solid curves) and in the dark (dashed curves). (**b**) OCP obtained from TiO_2 on pristine Au/TiO_2 heterostructures (black) and catechol-modified Au/TiO_2 heterostructures (red). The light was turned on at 10 s and off at 70 s. (**c**) Scheme of charge separation and water oxidation on catechol-modified Au/TiO_2 heterostructures. (**d**) The reaction order of TiO_2-trapped holes in driving PEC water oxidation on

catechol-modified Au/TiO_2 heterostructures. All experiments were performed in the unbuffered solution with pH 7.0.

Molecular redox adsorbates have been demonstrated to trap and stabilize photo-generated hot holes.[43-44] For driving multi-hole reactions, adsorbates need to be redox-active and also stable under water-oxidation conditions.[3] Catechol, a reductive form of quinone derivatives that are commonly used as redox mediators in natural photosynthesis (PSII system)[45-46] and metal-organic complexes,[44, 47-48] is expected to effectively store hot holes and assist multi-hole reactions when it adsorbs on Au surfaces in Au/TiO_2 heterostructures.

Catechol was photoelectrodeposited on Au/TiO_2 heterostructures (Supplementary Note 6 and Figure S23 to S25). Upon visible-light illumination, photo-generated hot holes oxidized catechol monomers and induced the oligomerization to form oligo-catechol on Au surfaces, which further trapped hot holes via a one-hole process of oxidizing the hydroxyl group (C–OH) to the ketone group (C=O) (Table S5 and Figure S26). In LSV measurements, the deposited catechol increased the photocurrent at 1.2 V_{RHE} from 47 μA to 84 μA (Figure 2a and Figure S27), showing an ~ 80% enhancement in PEC water oxidation. Meanwhile, the onset potential of LSV curve anodically shifted by ~ 60 mV (Figure 2a), suggesting that new active sites were generated upon the adsorption of catechol. The reproducibility of the photocurrent enhancement was discussed in Figure S28. In contrast to the enhanced photocurrent, V_{ph} on TiO_2 of the catechol-modified Au/TiO_2 was significantly suppressed (Figure 2b) while V_{ph} on Au was enhanced (Figure S29). This observation indicated that a portion of hot holes was directly trapped by catechol on Au but not transferred to TiO_2 (Figure 2c), consistent with the positive Au (binding energy of Au $4f_{7/2}$ = 84.8 ± 0.1 eV) in the XPS spectrum (Figure S30). It is also noted that EIS measurements showed a decreased capacitance of trapped holes on TiO_2 after the deposition of catechol (Figure S31),

affirming that fewer hot holes were transferred to TiO_2 (Supplementary Note 7, and Figure S32 and S33).

The adsorption of catechol on Au/TiO_2 heterostructures was further found to lower the reaction order of TiO_2-trapped holes in PEC water oxidation. When RDS only involved TiO_2-trapped holes, the reaction order of TiO_2-trapped holes was 2 (Figure 1c). However, once catechol-trapped holes were involved in RDS, the reaction order of TiO_2-trapped holes dropped to ~ 0.5 (Figure 2d and Figure S34). This significant change indicated that statistically fewer TiO_2-trapped holes participated in RDS of water oxidation when compared to those on the pristine Au/TiO_2. The rate law analysis (Supplementary Note 8) predicted a reaction order of 1 for TiO_2-trapped holes when RDS involved one TiO_2-trapped hole and one catechol-trapped hole. To further obtain a reaction order below 1, RDS should involve multiple elementary steps and at least one of them does not involve TiO_2-trapped holes. Therefore, catechol molecules adsorbed on Au should introduce a new reaction pathway for water oxidation (Figure 2c).

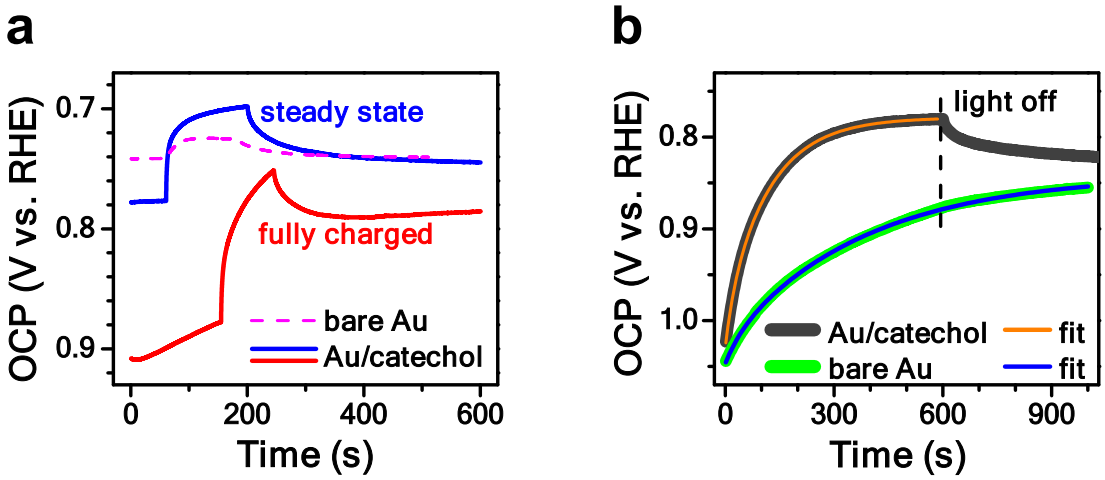

Figure 3. The Hot-hole releasing dynamics on catechol-modified Au. (**a**) OCP measurements of bare and catechol-modified Au NP electrodes. (**b**) OCP measurements immediately after the

bare and catechol-modified Au NP electrodes were fully charged under 470 nm illumination at 1.2 V_{RHE}. The light was turned off at 600 s. The OCP curves were fitted using the exponential decay equation (see Supplementary note 1).

Figure 1c showed that RDS of visible-light-driven water oxidation required two holes under neutral conditions. Although one catechol has two hydroxyl groups and the redox of each hydroxyl group can trap one hole, the weak oxidative capability of semiquinone made it difficult to have two C=O units work together to provide two holes for driving water oxidation (Figure S35a).[48-50] Thus, the two-hole RDS should happen either via sequential oxidations of one hydroxyl group of catechol (Figure S35 b and c) or through the cooperation between holes initially trapped on catechol and holes newly generated on Au (Figure S35d).

Those two reaction pathways can be distinguished by looking into the hot-hole trapping and releasing on Au as only the cooperation pathway involved newly generated holes on Au in RDS. Figure 3a showed that the Au/catechol electrode (catechol was photoelectrodeposited on a Au NP electrode, Supplementary Note 9 and Figure S36) that was fully charged by hot holes (i.e., all hydroxyl groups were oxidized to ketone groups, Figure S37) exhibited a much larger V_{ph} (~ 100 mV) than that on the bare Au NP electrode (20 mV), indicating the greatly enhanced electron-hole separation induced by adsorbed catechol. The subsequent decay of V_{ph} on the Au/catechol electrode (~ 70 mV at steady state, Figure 3a) implied an automatic release of trapped holes via reacting with water. To monitor the hole-releasing dynamics, OCP measurements were performed immediately after electrodes were fully charged with hot holes (Figure 3b). A fast decay of OCP towards the cathodic direction was observed (the grey curve in Figure 3b) and the fitting of OCP curve using the exponential decay equation (the orange curve in Figure 3b) showed timescales of 23 s and 119 s. In contrast, the bare Au NP electrode showed a much slower decay of OCP (the

green curve in Figure 3b) with timescales of 44 s and 379 s (the blue curve in Figure 3b), indicating a slow recovery of Au surfaces from oxidized Au.[51] The oxidized Au can be considered as a form of "inactive" surface-trapped holes that were unable to be released to oxidize water before energy dissipation, leading to the low water-oxidation activity on the bare Au surface (Figure S3). Thus, the catechol-accelerated hole releasing dynamics on Au suggested that initially "inactive" surface-trapped holes (oxidized Au) were "activated" by catechol-trapped holes and then those adjacent trapped holes worked cooperatively for driving water oxidation.

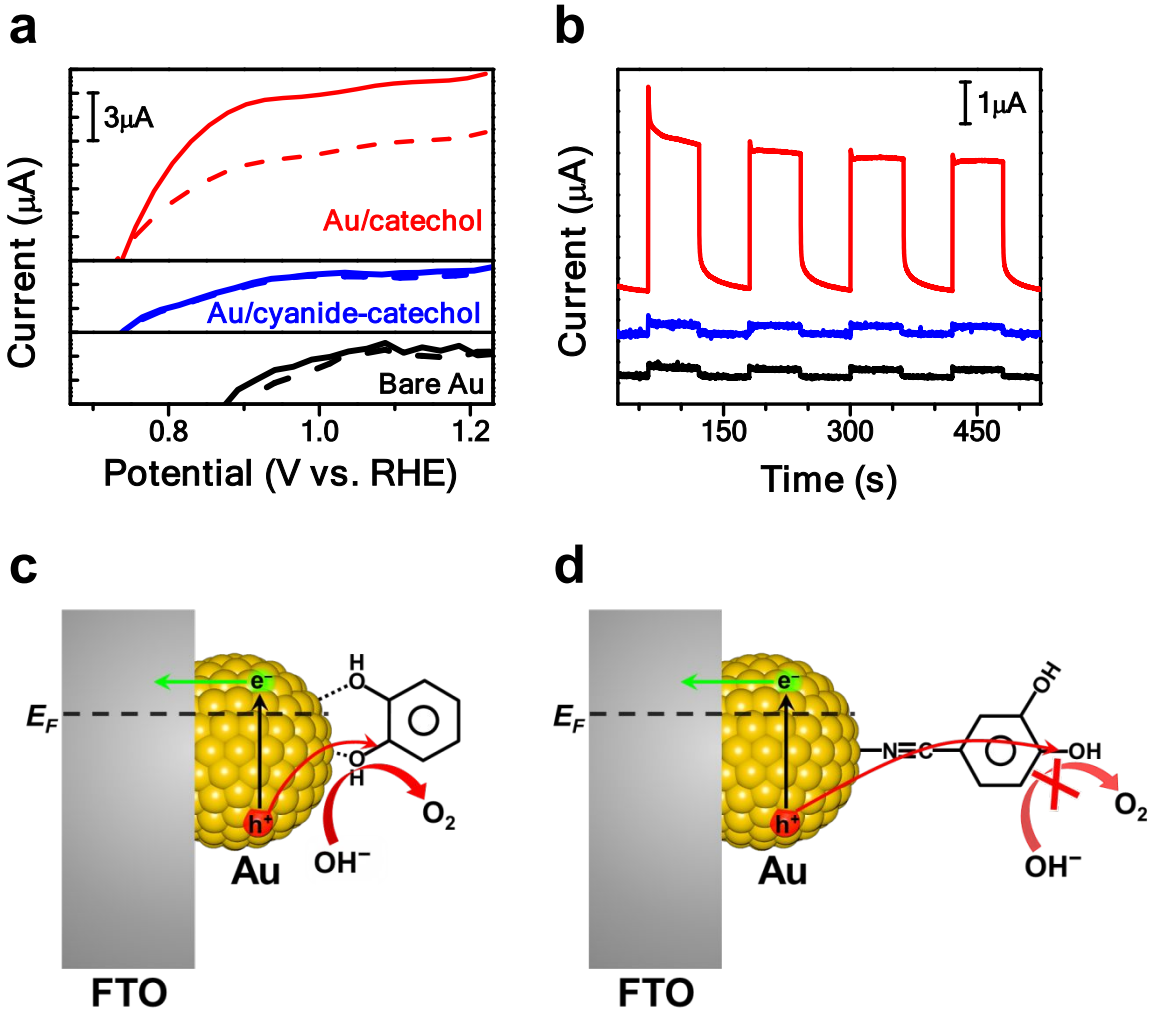

Figure 4. Water oxidation on catechol-modified Au NP electrodes. (**a**) LSV curves of bare, catechol-modified, and cyanide-catechol-modified Au NP electrodes under 470 nm illumination (solid curves) and in the dark (dashed curves) in the unbuffered solution with pH 7.0. (**b**) The corresponding chronoamperometry measurements at 1.2 V_{RHE} under chopped light illumination with 60 s interval. (**c**) Scheme of trapping hot holes on catechol-modified Au NP. Catechol confined hot holes at Au/catechol interfaces and facilitated water oxidation. (**d**) Scheme of trapping holes on cyanide-catechol-modified Au NP. In contrast to (**c**), cyanide-catechol transferred hot holes away from Au surfaces and blocked water oxidation.

As shown in Figure S35d, this cooperation pathway required the hole-trapping site to be on Au surfaces that also worked as the active site. In order to identify the role of Au surfaces in water oxidation, catechol molecules were modified with the cyanide group (i.e., 3,4-dihydroxybenzonitrile) to spatially separate the hole-trapping site (hydroxyl groups) away from Au surfaces (Figure 4d, Supplementary Note 10, and Figure S38 and S39) as the cyanide group adsorbs on Au stronger than the hydroxyl group.[52] LSV measurements showed that the onset potential of Au/cyanide-catechol electrode was cathodically shifted by 150 mV when compared with the bare Au NP electrode (Figure 4a), indicating that hot holes were able to be trapped on hydroxyl groups on the Au/cyanide-catechol electrode (Figure 4d). However, the photo-response on this electrode was found to be negligible (Figure 4a). Chronoamperometry (I-t) measurements further demonstrated that the Au/cyanide-catechol electrode only produced a photocurrent of 0.21 μA, which was comparable to that of the bare Au NP electrode (0.17 μA) (Figure 4b). Taken together, the low photocurrent response from Au/cyanide-catechol electrode strongly suggested that hot holes trapped at hydroxyl groups alone were not able to drive water oxidation. Instead, Au

surfaces were necessarily needed in water oxidation by providing active sites. Therefore, those trapped holes should be located at Au/catechol interfaces.

LSV measurements on the Au/catechol electrode showed a largely enhanced photo-response (red curves in Figure 4a) when compared to the bare Au NP electrode (black curves in Figure 4a). I-t measurement at 1.2 V_{RHE} further confirmed that the photocurrent on Au/catechol electrode was boosted by one order of magnitude (3.28 μA, Figure 4b) compared with that on the bare Au NP electrode (0.17 μA, Figure 4b). The reproducibility of the photocurrent enhancement was discussed in Figure S40. The faradaic efficiency of the evolved oxygen was measured to be 86% (Figure S41). All these results confirmed that hot holes trapped at Au/catechol interfaces were capable of driving water oxidation (Figure 4c, Supplementary Note 11, and Figure S40 to S44). As illustrated in Figure 5, both Au surfaces and catechol initially resided at their reduced states (i.e., Au (0) and C–OH bond, step I in Figure 5). The first transferred hot hole oxidized C–OH to C=O (step II in Figure 5), which was treated as a long-lived trapped hole. Another hole oxidized Au (adjacent to the formed C=O) and led to the formation of Au–OH (step III in Figure 5). The cooperation of C=O and Au–OH then led to the rate-limiting O–O formation that produced Au–OOH (step IV in Figure 5). Photo-excited holes in step IV and V maintained catechol at the oxidized state (in the form of C=O). Catechol-trapped hot holes further oxidized Au–OOH and released O_2 to complete water oxidation (steps V and VI in Figure 5). The reversible process between quinone and hydroquinone was supported by photocurrent recovery as shown in Figure S45. As a proof-of-concept, the multi-hole cooperation mechanism has been confirmed to be an effective strategy for driving water oxidation. Further improvement of water oxidation activity can be realized by material designs, such as controlling the morphology and facets of Au nanoparticles for exposing more adsorption and active sites.

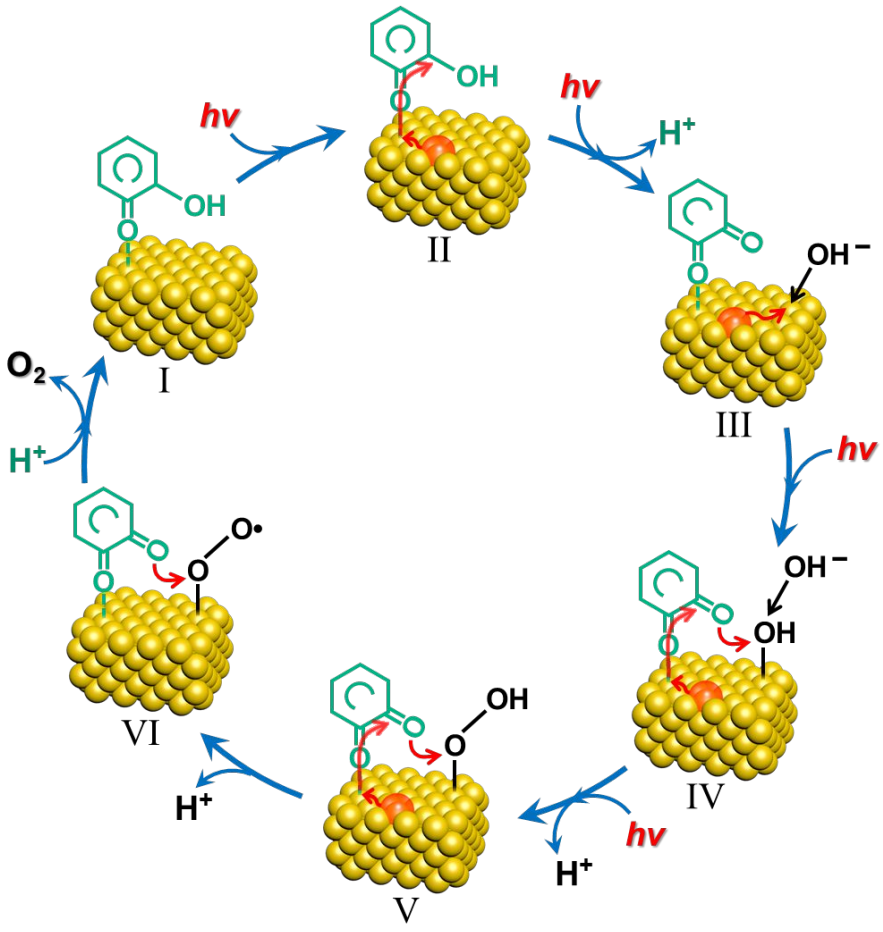

Figure 5. Proposed scheme of multi-hole cooperation pathway for water oxidation on catechol-modified Au surfaces. Red arrows indicated directions of hot-hole transfer. For simplicity, only one catechol molecule was shown to represent oligo-catechol.

Conclusion

We have successfully developed a molecular approach to stabilize photo-generated hot holes on Au/TiO_2 heterostructures for driving water oxidation under visible-light illumination. Since water oxidation represents a typical type of slow chemical reactions driven by multiple charge

carriers, it is expected that the newly created reaction pathway, the multi-hole cooperation, would be extendable to various multi-hole (or -electron) photochemical reactions at metal/semiconductor or metal/molecule interfaces. Taken together, our studies provide a molecular-level understanding of hot-hole-induced photocatalysis, highlighting the visible-light-mediated multi-hole collaboration as a new avenue for facilitating photochemical processes.

References and Notes

1. Le Formal, F.; Pastor, E.; Tilley, S. D.; Mesa, C. A.; Pendlebury, S. R.; Grätzel, M.; Durrant, J. R., Rate Law Analysis of Water Oxidation on a Hematite Surface. J. Am. Chem. Soc. **2015,** *137*, 6629-6637.

2. Zhang, Y.; Zhang, H.; Liu, A.; Chen, C.; Song, W.; Zhao, J., Rate-Limiting O–O Bond Formation Pathways for Water Oxidation on Hematite Photoanode. J. Am. Chem. Soc. **2018,** *140*, 3264-3269.

3. Chen, H.-Y.; Ardo, S., Direct observation of sequential oxidations of a titania-bound molecular proxy catalyst generated through illumination of molecular sensitizers. Nat. Chem. **2018,** *10*, 17-23.

4. Beiler, A. M.; Moore, G. F., Caught in the act. Nat. Chem. **2017,** *10*, 3.

5. Mesa, C. A.; Kafizas, A.; Francàs, L.; Pendlebury, S. R.; Pastor, E.; Ma, Y.; Le Formal, F.; Mayer, M. T.; Grätzel, M.; Durrant, J. R., Kinetics of Photoelectrochemical Oxidation of Methanol on Hematite Photoanodes. J. Am. Chem. Soc. **2017,** *139*, 11537-11543.

6. Inoue, H.; Shimada, T.; Kou, Y.; Nabetani, Y.; Masui, D.; Takagi, S.; Tachibana, H., The Water Oxidation Bottleneck in Artificial Photosynthesis: How Can We Get Through It? An Alternative Route Involving a Two-Electron Process. ChemSusChem **2011,** *4*, 173-179.

7. Anson, C. W.; Stahl, S. S., Cooperative Electrocatalytic O_2 Reduction Involving Co(salophen) with p-Hydroquinone as an Electron–Proton Transfer Mediator. J. Am. Chem. Soc. **2017,** *139*, 18472-18475.

8. Christopher, P.; Moskovits, M., Hot Charge Carrier Transmission from Plasmonic Nanostructures. Annu. Rev. Phys. Chem. **2017,** *68*, 379-398.

9. Zhang, Y.; He, S.; Guo, W.; Hu, Y.; Huang, J.; Mulcahy, J. R.; Wei, W. D., Surface-Plasmon-Driven Hot Electron Photochemistry. Chem. Rev. **2018,** *118*, 2927-2954.

10. Linic, S.; Christopher, P.; Ingram, D. B., Plasmonic-metal nanostructures for efficient conversion of solar to chemical energy. Nat. Mater. **2011,** *10*, 911-921.

11. Brongersma, M. L.; Halas, N. J.; Nordlander, P., Plasmon-induced hot carrier science and technology. Nat. Nanotechnol. **2015,** *10*, 25-34.

12. Aslam, U.; Rao, V. G.; Chavez, S.; Linic, S., Catalytic conversion of solar to chemical energy on plasmonic metal nanostructures. Nat. Catal. **2018,** *1*, 656-665.

13. Kazuma, E.; Jung, J.; Ueba, H.; Trenary, M.; Kim, Y., Real-space and real-time observation of a plasmon-induced chemical reaction of a single molecule. Science **2018,** *360*, 521-526.

14. Knight, M. W.; Sobhani, H.; Nordlander, P.; Halas, N. J., Photodetection with Active Optical Antennas. Science **2011,** *332*, 702-704.

15. Zhou, L.; Swearer, D. F.; Zhang, C.; Robatjazi, H.; Zhao, H.; Henderson, L.; Dong, L.; Christopher, P.; Carter, E. A.; Nordlander, P.; Halas, N. J., Quantifying hot carrier and thermal contributions in plasmonic photocatalysis. Science **2018,** *362*, 69-72.

16. Mubeen, S.; Lee, J.; Singh, N.; Kramer, S.; Stucky, G. D.; Moskovits, M., An autonomous photosynthetic device in which all charge carriers derive from surface plasmons. Nat. Nanotechnol. **2013,** *8*, 247-251.

17. Zhang, Y.; Yam, C.; Schatz, G. C., Fundamental Limitations to Plasmonic Hot-Carrier Solar Cells. J. Phys. Chem. Lett. **2016,** *7*, 1852-1858.

18. Brus, L., Noble Metal Nanocrystals: Plasmon Electron Transfer Photochemistry and Single-Molecule Raman Spectroscopy. Acc. Chem. Res. **2008,** *41*, 1742-1749.

19. Sundararaman, R.; Narang, P.; Jermyn, A. S.; Goddard Iii, W. A.; Atwater, H. A., Theoretical predictions for hot-carrier generation from surface plasmon decay. Nat. Commun. **2014,** *5*, 5788.

20. Hu, C.; Chen, X.; Jin, J.; Han, Y.; Chen, S.; Ju, H.; Cai, J.; Qiu, Y.; Gao, C.; Wang, C.; Qi, Z.; Long, R.; Song, L.; Liu, Z.; Xiong, Y., Surface Plasmon Enabling Nitrogen Fixation in Pure Water through a Dissociative Mechanism under Mild Conditions. J. Am. Chem. Soc. **2019,** *141*, 7807-7814.

21. Zandi, O.; Agrawal, A.; Shearer, A. B.; Reimnitz, L. C.; Dahlman, C. J.; Staller, C. M.; Milliron, D. J., Impacts of surface depletion on the plasmonic properties of doped semiconductor nanocrystals. Nat. Mater. **2018,** *17*, 710-717.

22. Tan, S.; Argondizzo, A.; Ren, J.; Liu, L.; Zhao, J.; Petek, H., Plasmonic coupling at a metal/semiconductor interface. Nat. Photonics **2017,** *11*, 806-812.

23. Shi, X.; Ueno, K.; Oshikiri, T.; Sun, Q.; Sasaki, K.; Misawa, H., Enhanced water splitting under modal strong coupling conditions. Nat. Nanotechnol. **2018,** *13*, 953-958.

24. Kim, Y.; Smith, J. G.; Jain, P. K., Harvesting multiple electron–hole pairs generated through plasmonic excitation of Au nanoparticles. Nat. Chem. **2018,** *10*, 763-769.

25. Zhan, C.; Chen, X.-J.; Yi, J.; Li, J.-F.; Wu, D.-Y.; Tian, Z.-Q., From plasmon-enhanced molecular spectroscopy to plasmon-mediated chemical reactions. Nat. Rev. Chem. **2018,** *2*, 216-230.

26. Yang, W.-C. D.; Wang, C.; Fredin, L. A.; Lin, P. A.; Shimomoto, L.; Lezec, H. J.; Sharma, R., Site-selective CO disproportionation mediated by localized surface plasmon resonance excited by electron beam. Nat. Mater. **2019,** *18*, 614–619.

27. Zhai, Y.; DuChene, J. S.; Wang, Y.-C.; Qiu, J.; Johnston-Peck, A. C.; You, B.; Guo, W.; DiCiaccio, B.; Qian, K.; Zhao, E. W.; Ooi, F.; Hu, D.; Su, D.; Stach, E. A.; Zhu, Z.; Wei, W. D., Polyvinylpyrrolidone-induced anisotropic growth of gold nanoprisms in plasmon-driven synthesis. Nat. Mater. **2016,** *15*, 889-895.

28. Polte, J.; Erler, R.; Thünemann, A. F.; Sokolov, S.; Ahner, T. T.; Rademann, K.; Emmerling, F.; Kraehnert, R., Nucleation and Growth of Gold Nanoparticles Studied via in situ Small Angle X-ray Scattering at Millisecond Time Resolution. ACS Nano **2010,** *4*, 1076-1082.

29. Le Formal, F.; Pendlebury, S. R.; Cornuz, M.; Tilley, S. D.; Grätzel, M.; Durrant, J. R., Back Electron–Hole Recombination in Hematite Photoanodes for Water Splitting. J. Am. Chem. Soc. **2014,** *136*, 2564-2574.

30. Wang, J.; Ding, T.; Wu, K., Charge Transfer from n-Doped Nanocrystals: Mimicking Intermediate Events in Multielectron Photocatalysis. J. Am. Chem. Soc. **2018,** *140*, 7791-7794.

31. Wang, J.; Ding, T.; Wu, K., Electron Transfer into Electron-Accumulated Nanocrystals: Mimicking Intermediate Events in Multielectron Photocatalysis II. J. Am. Chem. Soc. **2018,** *140*, 10117-10120.

32. DuChene, J. S.; Sweeny, B. C.; Johnston-Peck, A. C.; Su, D.; Stach, E. A.; Wei, W. D., Prolonged Hot Electron Dynamics in Plasmonic-Metal/Semiconductor Heterostructures with Implications for Solar Photocatalysis. Angew. Chem. Int. Ed. **2014,** *53*, 7887-7891.

33. Furube, A.; Du, L.; Hara, K.; Katoh, R.; Tachiya, M., Ultrafast Plasmon-Induced Electron Transfer from Gold Nanodots into TiO_2 Nanoparticles. J. Am. Chem. Soc. **2007,** *129*, 14852-14853.

34. Jia, H.; Du, A.; Zhang, H.; Yang, J.; Jiang, R.; Wang, J.; Zhang, C.-y., Site-Selective Growth of Crystalline Ceria with Oxygen Vacancies on Gold Nanocrystals for Near-Infrared Nitrogen Photofixation. J. Am. Chem. Soc. **2019,** *141*, 5083-5086.

35. Wang, S.; Gao, Y.; Miao, S.; Liu, T.; Mu, L.; Li, R.; Fan, F.; Li, C., Positioning the Water Oxidation Reaction Sites in Plasmonic Photocatalysts. J. Am. Chem. Soc. **2017,** *139*, 11771-11778.

36. Liu, G.; Zhen, C.; Kang, Y.; Wang, L.; Cheng, H.-M., Unique physicochemical properties of two-dimensional light absorbers facilitating photocatalysis. Chem. Soc. Rev. **2018,** *47*, 6410-6444.

37. Chen, R.; Pang, S.; An, H.; Zhu, J.; Ye, S.; Gao, Y.; Fan, F.; Li, C., Charge separation via asymmetric illumination in photocatalytic Cu_2O particles. Nat. Energy **2018,** *3*, 655–663.

38. Urso, C.; Barawi, M.; Gaspari, R.; Sirigu, G.; Kriegel, I.; Zavelani-Rossi, M.; Scotognella, F.; Manca, M.; Prato, M.; De Trizio, L.; Manna, L., Colloidal Synthesis of Bipolar Off-Stoichiometric Gallium Iron Oxide Spinel-Type Nanocrystals with Near-IR Plasmon Resonance. J. Am. Chem. Soc. **2016,** *139*, 1198–1206.

39. Zhang, Y.; Zhang, H.; Ji, H.; Ma, W.; Chen, C.; Zhao, J., Pivotal Role and Regulation of Proton Transfer in Water Oxidation on Hematite Photoanodes. J. Am. Chem. Soc. **2016,** *138*, 2705-2711.

40. Kim, Y.-S.; Kriegel, S.; Harris, K. D.; Costentin, C.; Limoges, B.; Balland, V., Evidencing Fast, Massive, and Reversible H+ Insertion in Nanostructured TiO_2 Electrodes at Neutral pH. Where Do Protons Come From? J. Phys. Chem. C **2017,** *121*, 10325-10335.

41. Klahr, B.; Gimenez, S.; Fabregat-Santiago, F.; Bisquert, J.; Hamann, T. W., Electrochemical and photoelectrochemical investigation of water oxidation with hematite electrodes. Energy Environ. Sci. **2012,** *5*, 7626-7636.

42. You, B.; Sun, Y., Innovative Strategies for Electrocatalytic Water Splitting. Acc. Chem. Res. 2018, 51, 1571-1580.

43. La Croix, A. D.; O'Hara, A.; Reid, K. R.; Orfield, N. J.; Pantelides, S. T.; Rosenthal, S. J.; Macdonald, J. E., Design of a Hole Trapping Ligand. Nano Lett. **2017,** *17*, 909-914.

44. Tachan, Z.; Hod, I.; Zaban, A., The TiO2–Catechol Complex: Coupling Type II Sensitization with Efficient Catalysis of Water Oxidation. Adv. Eng. Mater. **2014,** *4*, 1301249.

45. Rappaport, F.; Diner, B. A., Primary photochemistry and energetics leading to the oxidation of the $(Mn)_4Ca$ cluster and to the evolution of molecular oxygen in Photosystem II. Coord. Chem. Rev. **2008,** *252*, 259-272.

46. Kato, M.; Cardona, T.; Rutherford, A. W.; Reisner, E., Photoelectrochemical Water Oxidation with Photosystem II Integrated in a Mesoporous Indium–Tin Oxide Electrode. J. Am. Chem. Soc. **2012,** *134*, 8332-8335.

47. Wada, T.; Tsuge, K.; Tanaka, K., Electrochemical oxidation of water to dioxygen catalyzed by the oxidized form of the bis(ruthenium-hydroxo) complex in H_2O. Angew. Chem. Int. Ed. **2000,** *39*, 1479-1481.

48. Tanaka, K.; Isobe, H.; Yamanaka, S.; Yamaguchi, K., Similarities of artificial photosystems by ruthenium oxo complexes and native water splitting systems. Proc. Natl Acad. Sci. **2012,** *109*, 15600-15605.

49. Wada, T.; Tsuge, K.; Tanaka, K., Syntheses and Redox Properties of Bis(hydroxoruthenium) Complexes with Quinone and Bipyridine Ligands. Water-Oxidation Catalysis. Inorg. Chem. **2001,** *40*, 329-337.

50. Muckerman, J. T.; Polyansky, D. E.; Wada, T.; Tanaka, K.; Fujita, E., Water Oxidation by a Ruthenium Complex with Noninnocent Quinone Ligands: Possible Formation of an O−O Bond at a Low Oxidation State of the Metal. Inorg. Chem. **2008,** *47*, 1787-1802.

51. Wang, P.; Krasavin, A. V.; Nasir, M. E.; Dickson, W.; Zayats, A. V., Reactive tunnel junctions in electrically driven plasmonic nanorod metamaterials. Nat. Nanotechnol. **2018,** *13*, 159-164.

52. Guttentag, A. I.; Wächter, T.; Barr, K. K.; Abendroth, J. M.; Song, T.-B.; Sullivan, N. F.; Yang, Y.; Allara, D. L.; Zharnikov, M.; Weiss, P. S., Surface Structure and Electron Transfer Dynamics of the Self-Assembly of Cyanide on Au{111}. J. Phys. Chem. C **2016,** *120*, 26736-26746.

Acknowledgments

Funding: This work is supported by the National Science Foundation under Grant CHE-1808539, DMR-1352328, and the CCI Center for Nanostructured Electronic Materials (CHE-1038015). Materials characterization was conducted at MAIC and NRF, College of Engineering Research Service Centers, University of Florida. XPS characterization was conducted using an instrument purchased with NSF grant MRI-DMR-1126115. LC-MS characterization was conducted in the Mass Spectrometry Research and Education Center funded with NIH grant S10OD021758-01A1. STEM characterization used resources of the Center for Functional Nanomaterials, which is a U.S. DOE Office of Science Facility, at Brookhaven National Laboratory under Contract No. DE-SC0012704. W.G. acknowledges the support of a graduate school fellowship from UF and the DOE Science Graduate Student Research (SCGSR) Award. Y. Zhang greatly appreciates the

support from Ann Stasch Summer Fellowship, Vala Research Excellence Award, and College of Liberal Art and Science (CLAS) Dissertation Fellowship funded by the Charles Vincent and Heidi Cole McLaughlin Endowment. **Author contributions:** W.D.W. and Y.C.Z. conceived the idea and designed experiments. Y.C.Z. and Y.L.Z. synthesized materials. Y.C.Z. conducted electrochemical studies. Y.L.Z. conducted UV-vis experiments. W.X.G. performed XPS experiments. A.C.J.-P. and W.X.G. conducted electron microscopy characterization. X.N.S conducted LC-MS experiments. Y.H. participated in the discussion. Y.C.Z. and W.D.W. wrote the manuscript with contributions from all authors. W.D.W. supervised the project. **Competing interests:** Authors declare no competing interests. **Data and materials availability:** All data are available in the manuscript and in the supplementary materials.

Present Address

§ Key Laboratory of Photochemistry, CAS Research/Education Center for Excellence in Molecular Sciences, Institute of Chemistry, Chinese Academy of Sciences, Beijing 100190, P. R. China